Rapamycin increases murine lifespan but does not reduce mineral volume in the Matrix GLA Protein (MGP) knockout mouse model of medial arterial calcification.

Parya Behzadi[1], Rolando A. Cuevas[1], Alex Crane[1], Andrew A Wendling[1], Claire C. Chu[1], William J Moorhead III[1], Ryan Wong[1], Mark Brown[1], Joshua Tamakloe[1], Swathi Suresh[1], Payam Salehi[2], Iris Z. Jaffe[3], Allison L. Kuipers[4], Lyudmila Lukashova[5], Konstantinos Verdelis[5], and Cynthia St. Hilaire[1, 6]

[1] Department of Medicine, Division of Cardiology, and the Pittsburgh Heart, Lung, Blood and Vascular Medicine Institute, University of Pittsburgh, Pittsburgh, Pennsylvania, USA.

[2] CardioVascular Center, Vascular Surgery, Tufts Medical Center, 800 Washington Street, Boston, MA, 02111-1800, USA

[3] Molecular Cardiology Research Institute, Tufts Medical Center, 800 Washington Street, Boston, MA, 02111-1800, USA

[4] Department of Epidemiology, School of Public Health, University of Pittsburgh, Pittsburgh, Pennsylvania, USA.

[5] Departments of Endodontics and Oral Biology, School of Dental Medicine, University of Pittsburgh, Pittsburgh, PA, USA

[6] Department of Bioengineering, University of Pittsburgh, Pittsburgh, Pennsylvania, USA.

ABSTRACT: 235 words

MANUSCRIPT:

KEYWORDS: Medial Arterial Calcification, Rapamycin, Matrix GLA protein

ABBREVIATIONS

Adenosine monophosphate	AMP
Adenosine triphosphate	ATP
Alkaline phosphate	TNAP
Arterial calcification due to deficiency of CD73	ACDC
Ecto-5'-nucleotidase	NT5E
Induced pluripotent stem cells	iPSCs
Matrix GLA protein	MGP
Medial arterial calcification	MAC
mTORC complex 1	mTORC1
mTORC complex 2	mTORC2
Peripheral artery disease	PAD
Smooth muscle α-actin	SMA
Smooth muscle cells	SMCs
Myosin heavy chain 11	MYH11
Runt-related transcription factor 2	RUNX2

ABSTRACT

Peripheral artery disease (PAD) is the narrowing of the arteries that carry blood to the lower extremities. PAD has been traditionally associated with atherosclerosis. However, recent

studies have found that medial arterial calcification (MAC) is the primary cause of chronic limb ischemia below the knee. MAC involves calcification of the elastin fibers surrounding smooth muscle cells (SMCs) in arteries. Matrix GLA Protein (MGP) binds circulating calcium and inhibits vascular calcification. *Mgp*$^{-/-}$ mice develop severe MAC and die within 8 weeks of birth due to aortic rupture or heart failure. We previously discovered a rare genetic disease Arterial Calcification due to Deficiency in CD73 (ACDC) in which patients present with extensive MAC in their lower extremity arteries. Using a patient-specific induced pluripotent stem cell model we found that rapamycin inhibited calcification. Here we investigated whether rapamycin could reduce MAC in vivo using *Mgp*$^{-/-}$ mice as a model. *Mgp*$^{+/+}$ and *Mgp*$^{-/-}$ mice received 5mg/kg rapamycin or vehicle. Calcification content was assessed via microCT, and vascular morphology and extracellular matrix content assessed histologically. Immunostaining and western blot analysis were used to examine SMC phenotypes and cellular functions. Rapamycin prolonged *Mgp*$^{-/-}$ mice lifespan, decreased mineral density in the arteries, and increased smooth muscle actin protein levels, however, calcification volume, vessel morphology, SMC proliferation, and autophagy flux were all unchanged. These findings suggest that rapamycin's effects in the *Mgp*$^{-/-}$ mouse are independent of the vascular phenotype.

INTRODUCTION

Peripheral artery disease (PAD) is the narrowing of blood vessels in the lower extremities due to inward remodeling or thrombotic occlusion, both of which cause chronic limb ischemia and often result in amputation of the lower leg (1). Traditionally atherosclerosis was the assumed cause of PAD however recent studies now show that medial arterial calcification (MAC) promotes inward remodeling, and stiffness related to medial dysplasia induces thrombosis (2-4). MAC is characterized by the progressive buildup of calcium and phosphate within the arterial walls and is typically not associated with lipid deposition, fibrous cap formation, or intimal hyperplasia (5). These structural features distinguish MAC from atherosclerosis and indicate that MAC is a distinct pathology driving adverse outcomes in PAD. Currently, there are no specific medical therapies that target the pathogenesis of PAD or MAC. Finding therapies that can prevent, stop, or even reverse MAC in PAD could greatly enhance the current standard of care.

Vascular calcification stems from the nucleation of calcium and phosphate into hydroxyapatite crystals and the release of pro-mineralizing matrix vesicles from osteogenic-like arterial smooth muscle cells (SMCs) that accumulate along the elastic lamina (6). Phosphate is a byproduct of the breakdown of extracellular adenosine triphosphate (ATP) to adenosine, generating inorganic phosphate at several points (7, 8). There are a number of genetic diseases that present with MAC which harbor inactivating mutations in the genes related to extracellular ATP metabolism (5). Patients with Arterial Calcification due to Deficiency of CD73 (ACDC, also known as CALJA, OMIM # 211800) harbor inactivating mutations in the *NT5E* gene, which encodes for the CD73 enzyme that metabolizes extracellular AMP to adenosine and inorganic phosphate. Key signatures of this disease are calcification nodules in the small joint capsules and MAC in the lower-extremity arteries that initiate along the elastic lamina (4, 9, 10). We previously found that a lack of CD73-mediated adenosine enhanced the expression and activity of tissue-nonspecific alkaline phosphatase (TNAP), a key enzyme that promotes calcification (11).

Matrix GLA protein (MGP) is a vitamin-K2-dependent protein with an unusual gamma-carboxylation of five glutamate residues that enhance its affinity for calcium, preventing it from mineralizing (12). MGP also inhibits calcification propagation by binding to hydroxyapatite crystals and stimulating their uptake by local phagocytosing macrophages (13). MGP also modulates osteogenic signaling by binding to BMP-2, preventing it from activating receptors and upregulating RUNX2, the key regulator of osteoblast differentiation and maturation (14, 15). Mice that lack MGP develop to term but die prematurely within approximately two months of age

due to extensive MAC, which leads to aortic rupture or heart failure (16). Aortas of MGP-deficient mice exhibit increased collagen accumulation and elastin fiber fragmentation within the medial layer of the arteries where calcification is also localized. This is phenotypically similar to MAC observed in human patients with PAD MAC and ACDC patients (4).

The drug rapamycin inhibits the mammalian target of rapamycin (mTOR), a protein kinase broadly expressed throughout the body, which controls many key processes such as energy balance, autophagy, and proliferation (17-20). Rapamycin protects against the calcification of vascular cells in in vitro and ex vivo models, as well as in in vivo models of chronic kidney disease-induced MAC (21-23). We previously found rapamycin prevented calcification in in vitro and in vivo disease models of ACDC patient-specific induced pluripotent stem cells (iPSCs) (11).

While CD73-deficient humans develop extensive MAC in their lower extremity large vessels, CD73-deficient mice do not phenocopy humans and do not exhibit calcification in their vasculature.(24, 25) As the MAC observed in MGP-deficient mice mirrors that seen in ACDC patients, we sought to investigate whether rapamycin prevented calcification in this genetic mouse model of MAC.

MATERIALS AND METHODS

Availability of Materials

We abide by the NIH Grants Policy on Sharing of Unique Research Resources, including the NIH Policy on Sharing of Model Organisms for Biomedical Research (2004), NIH Grants Policy Statement (2003), and Sharing of Biomedical Research Resources: Principles and Guidelines for Recipients of NIH Grants and Contracts (1999), and the Bayh-Dole Act and the Technology Transfer Commercialization Act of 2000. Materials generated in our laboratory are made available for non-commercial research per established University of Pittsburgh Office of Research IRB and MTA protocols.

Institutional Review Board Statement

De-identified human tissues were obtained, with informed consent from subjects, who were enrolled in studies approved by the University of Pittsburgh or Tufts Medical Center institutional review boards, per the Declaration of Helsinki.

Animals and cell line generation

Animal use was approved by the Institutional Animal Care and Use Committee at the University of Pittsburgh. MGP heterozygous mutant mice from a C57BL/6J background (strain# 023811 Jackson Laboratory, Bar Harbor, ME) were bred to produce +/+ and -/- littermate controls. Smooth muscle lineage-specific *Raptor* (*Mgp*$^{-/-}$; *Raptor*$^{SMC-/-}$) and *Rictor* (*Mgp*$^{-/-}$; *Rictor*$^{SMC-/-}$) knockout mice were produced by breeding *Mgp*$^{+/-}$ with Myh11-Cre-eGFP mice (strain# 007742 Jackson Laboratory, Bar Harbor, ME)(26), with Raptor-LoxP (strain# 013188 Jackson Laboratory, Bar Harbor, ME)(27), or *Rictor*-LoxP (strain# 020649 Jackson Laboratory, Bar Harbor, ME)(28). Genotypes were determined from tail snips that were incubated in DirectPCR Lysis Reagent (Viagen Biotech) according to manufacturer instructions. The lysate was amplified using OneTaq MasterMix (New England Biolabs) according to manufacturer instructions with primers suggested by Jackson Laboratories. The PCR reaction was run on an ethidium bromide agarose gel. SMC were obtained from three- to five-week-old male and female *Mgp*$^{+/+}$ and *Mgp*$^{-/-}$ mice.

Cell culture

Mgp$^{+/+}$ and *Mgp*$^{-/-}$ aortic SMC lines from male and female murine aorta were cultured in Dulbecco's modified Eagle's medium (DMEM; Gibco, Waltham, MA) supplemented with 20% FBS (FBS; R&D Systems, Minneapolis, MN) and 100 U/mL penicillin-streptomycin (P/S; Gibco, Waltham, MA). Growth media was changed every three days, and cells were split 1:2 when confluent. Post-expansion, 25,000–50,000 cells/cm^2 were plated with serum reduced 10% FBS in DMEM medium and grown to confluence. Before all experiments/treatments, cells were serum-starved in DMEM with 0.5% FBS for 48 h. Incubation under reduced serum conditions has been proven to be a beneficial technique for studying smooth muscle cell remodeling and contractility in vitro (29, 30). Cells were treated with rapamycin (Novus Biologicals) at concentrations of 200 nM or the same volume of DMSO as vehicle control for 12h. For autophagy flux assessment, cells were exposed to either bafilomycin A1 100 nM (Sigma-Aldrich) or rapamycin 200 nM for a duration of 24h following treatment intervention. All chemicals were dissolved in DMSO and administered in equal volume as vehicle control.

Tissue Extraction

Mice were sacrificed by asphyxiation with carbon dioxide, followed by perforation of the diaphragm. Tissue extraction began with dissection through the abdominal wall and then perfusion of the heart with 50 mL of DPBS supplemented with 1:100 Amphotericin B (15290026, Gibco) and 1:200 Gentamicin (15710064, Gibco). The aortas were maintained in this solution while the adventitia was removed in a petri dish. Tissues were then fixed in 4% PFA in PBS for 2 hours and embedded in paraffin.

In Vivo Rapamycin Injections

Male and female *Mgp*$^{-/-}$ mice received intraperitoneal injections of either vehicle or 5 mg/kg rapamycin dissolved in 0.3 mg/ml peanut oil once a week beginning at 10 days of age. This process continued until the natural death of all mice in each group. To assess the volume and density of calcification, male and female *Mgp*$^{-/-}$ mice received intraperitoneal injections of either vehicle, 1x/week rapamycin or 3x/week rapamycin from 10 to 20 days of age.

Micro-Computed Tomography

A Scanco 30µCT microCT scanner (Scanco Medical, Bassersdorf, Switzerland) with a 45 kVp beam energy (1,000 ms exposure) was used to assess the volume and density of calcification in mouse aorta ex vivo, as previously described (11, 31). No filtering was used, allowing for visibility of lower CT densities. Images were then analyzed for relative calcified mass within the aorta (expressed as bone volume fraction) using the Scanco 3D Morphometry and Densitometry Analysis software (Scanco Medical) after binarization of the images with a global threshold within a user-defined aorta region of interest.

Western Blot Analysis

Cells were lysed in 1% CHAPS hydrate, 150 mmol/L sodium chloride, 25 mmol/L HEPES buffer supplemented with 1× protease and phosphatase inhibitor (Sigma-Aldrich). Cells were scraped into microcentrifuge tubes, vortexed for 5 minutes, freeze/thawed for 5 to 8 cycles, then centrifuged at 12□000×g for 10 minutes at 4°C. Supernatant protein concentration was determined using Pierce BCA protein assay kit (Thermo Fisher, Waltham, MA). Ten micrograms of protein were used in the preparation of lysate with 1 × Pierce LDS sample buffer nonreducing (Thermo Fisher, Waltham, MA) and 1 × NuPAGE sample reducing agent (Novex, Waltham, MA). Lysates were denatured at 95°C for 15 min and then electrophoresed on 4%–20% TGX stain-free polyacrylamide gel (Bio-Rad, Hercules, CA) in 1 × Tris/Glycine/SDS buffer (Bio-Rad, Hercules, CA) at 120 V for 50 min. Protein was transferred onto a 0.2 µm nitrocellulose membrane in prepared 1 × Towbin buffer with ethanol (EtOH) at 1 A and 25 V for 30 min using the Trans-Blot Turbo Transfer System (Bio-Rad, Hercules, CA). Membranes were blocked in 1:1

Odyssey blocking buffer (Li-COR, Lincoln, NE) and PBS for 1 h at room temperature, followed by primary antibody incubation in 1:1 Odyssey blocking buffer and PBS plus 0.1% Tween 20 (PBS-T) at 4°C overnight. Membranes were washed in PBS-T three times for 5 min, then incubated in secondary antibody at room temperature for 1 h. Membranes belonging to the same experimental set were imaged simultaneously on an Odyssey CLx (LI-COR, Lincoln, NE), and band intensity quantification was performed with Image Studio (Version 5.2, LI-COR, Lincoln, NE) software. Individual bands were normalized to α-tubulin, and each treatment group's fold change was compared with each gel's vehicle control lanes. For sequential antibody incubations, membranes were stripped in 1 × NewBlot Nitro Western Blot Stripping Buffer (LI-COR, Lincoln, NE) for 10 min, followed by three washes in PBS.

Verhoeff Van Gieson, Von Kossa and Masson's Trichrome Staining

Mice aortic tissues were removed from mice through a modified bilateral thoracosternotomy under anesthesia conditions. Then aortic tissue was fixed with 10% paraformaldehyde and embedded in paraffin. The embedded specimens were transversely sectioned at 10 µm on a microtome cryostat (Microm HM 325). Slides with the adhered paraffin aortic sections were warmed to 65°C for 1 h and then deparaffinized through xylene, rehydrated with serial incubation in graded alcohol baths, and stained with Verhoeff–van Gieson for elastic fiber visualization (Polysciences, 25089-1) or Von Kossa for calcification using the Von Kossa Method of Calcium Kit (Polysciences, 24633-1) and Masson's for collagen fibers (Polysciences, 25088-1), according to manufacturer's instructions. Images were captured using PreciPoint scanner. The thickness of the artery was measured using ImageJ software (Java 8), where the medial thickness was determined by measuring the distance between the inner and outer elastic lamina at four sites per vessel. Measurements were normalized to the scale bar of each picture. Data is shown as a total pixel's length. The length of elastic fibers was measured by selecting three random areas within the vessel and using ImageJ to trace and measure each fiber. Measurements were normalized to the area unit square.

Immunofluorescence

Slides with the adhered paraffin aortic sections were warmed to 65°C for 1 h and then deparaffinized through xylene, rehydrated with serial incubation in graded alcohol baths. Slides were boiled in citric acid-based antigen retrieval solution (H-3300, Vector Labs) for 20 minutes. Slides were cooled in the unmasking solution for 1 hour, washed in 1x PBS and placed in blocking buffer (500 mL PBS 0.3g Fish Skin Gelatin) for 1 hour. Tissues were incubated overnight at 4°C with antibodies for MYH11 (Abnova, mab34251, 1:50) and ACTA2 (Abcam, ab5694, 1:50), RUNX2 (ABclonal, A2851, 1:100), LC3 (cell signaling,124714, 1:50), Ki67 (Abcam, ab15580, 1:250). All signals were optimized to IgG (Vector, 31235, 1:50). Cells were washed 3× for 5 minutes each with PBS, 0.1% TWEEN 20, then once with PBS, and then incubated with secondary antibody (A11006, A11012, Thermo Fisher) for 1 hour. Cells were washed 3× for 5 minutes each with PBS, 0.1% TWEEN 20, then once with PBS, then mounted with Fluoroshield Mounting Medium with DAPI (Ab104139, Abcam). Slides were imaged within 24 hours of mounting. Cells were imaged within 24 hours of mounting. In ImageJ, each image was split into blue, red, and green channels, and the pixel intensity of the red and blue channels was measured (32). The measured intensity of a given stain was normalized to DAPI intensity of that same image. We obtained the von Kossa staining images using PreciPoint scanner and the immunofluorescent image using a Nikon NI-E I microscope.

Statistics

Statistical analysis was performed with GraphPad Prism 9.2 (GraphPad Software, Inc) and data shown are mean±SD. Statistical significance between groups was assessed using the Kruskal Wallis test or by Two-way ANOVA according to the data set. Statistical analysis used, exact n

values, biological replicates, and P values are stated within each figure legend. A p-value equal to or less than 0.05 will be considered statistically significant.

RESULTS

MAC in MGP-deficient mice phenocopies human MAC.

The main characteristic of MAC is calcification in the media along the elastic lamina. Von Kossa staining for calcification illustrates that *Mgp*$^{-/-}$ mouse aortas have extensive mineralization in the medial layer, which phenocopies the mineralization seen in MAC of the human tibial arteries and is distinct from neointimal calcification found in the necrotic core of coronary artery with atherosclerotic plaque (Figure 1A). MGP is a potent inhibitor of soft tissue calcification. *Mgp*$^{-/-}$ mice do not produce any MGP protein (Figure 1B) and, as a result, develop extensive MAC pathology in large vessels.

Rapamycin reduces mineral density in *Mgp*$^{-/-}$ mice.

It has been shown that the *Nt5e*-knockout mice model shows altered renal function, diminished control of the glomerular arteriolar tone, elevated atherogenesis, elevated thrombotic occlusion, and elevated hypoxia-induced vascular leakage.(24) However, they do not develop ectopic bone formation, do mimic the human vascular calcification phenotype, and do not have impaired formation of bone and teeth, while CD73-deficient ACDC patients develop extensive ectopic calcification (24, 25, 33). Jin et al. circumvented this issue using a patient-specific in vitro and in vivo disease modeling system using iPSC technology. They demonstrated that patient-specific ACDC-iPSCs developed extensive calcification in the in vivo teratoma model relative to control patient iPSCs. Furthermore, they found that treating mice bearing ACDC-iPSC teratomas with rapamycin reduced calcification (11).

As CD73-deficient mice do not sufficiently recapitulate the MAC observed in ACDC patients, here we used the *Mgp*$^{-/-}$ mice as an in vivo model of MAC. Mice were administered 5 mg/kg rapamycin injected three times per week starting at 10 days old until natural death (Figure 2A). We discovered that rapamycin treatment extended the lifespan of *Mgp*$^{-/-}$ mice (T_{50} 61 days) compared to the *Mgp*$^{-/-}$ mice treated with the DMSO vehicle (T_{50} 35 days), which start to die as early as day 20 (Figure 2B). Rapamycin's effects on extending lifespan has been observed in genetically heterogeneous non-diseased mice (34). Both male (n=11) and female (n=8) were used however no sex differences were observed between *Mgp*$^{-/-}$ mice that had received either vehicle or rapamycin treatment.

We also evaluated whether a low-frequency regime of rapamycin administration (one dose of 5 mg/kg injected weekly) versus a high-frequency regime of 5 mg/kg injected three times per week affected the *Mgp*$^{-/-}$ vascular mineral density at day 20, before natural death (Figure 3A). Whole aorta microCT analysis found no differences in the total calcification volume in either treatment regime; however, mice receiving a high regime of rapamycin exhibited decreased mineral density compared to the control group (Figure 3B). Von Kossa stain showed that the aortas of *Mgp*$^{+/+}$ mice exhibit no mineralization, while both vehicle- and rapamycin-treated *Mgp*$^{-/-}$ mice showed extensive calcification with no discernible differences between vehicle or rapamycin groups (Figure 3C). Medial wall thickness was not different between *Mgp*$^{+/+}$ and *Mgp*$^{-/-}$ that had received vehicle or rapamycin treatment (Figure 3C). RUNX2 is a key transcription factor promoting vascular cell osteogenic differentiation (6). Immunofluorescent staining revealed that while *Mgp*$^{-/-}$ mice showed elevated levels of RUNX2 compared to *Mgp*$^{+/+}$ mice, rapamycin treatment did not reduce RUNX2 expression in *Mgp*$^{-/-}$ compared to *Mgp*$^{-/-}$ treated with vehicle (Figure 3D). These findings suggest that while rapamycin doubles the lifespan of *Mgp*$^{-/-}$ mice, it has little to no effect in protecting the *Mgp*$^{-/-}$ mouse vasculature from calcification.

SMC phenotype remains unchanged after rapamycin treatment in vivo

The drug rapamycin has a broad spectrum of effects on SMCs. Rapamycin inhibits SMC migration and proliferation by inducing the cyclin-dependent kinase inhibitors $p27^{kip}$ and $p21^{cip}$ and promotes G1-S cell cycle arrest (35, 36). Rapamycin also induces SMC differentiation by inhibiting the mTOR-target S6K1 via AKT activation, promoting SMC contractile phenotype by enhancing SMA and MYH11 protein expression (37). Further, rapamycin was shown to protect against calcification of vascular cells in in vitro and ex vivo models (11, 21). While rapamycin did not reduce calcification volume in *Mgp*$^{-/-}$ vessels we hypothesized that it could perhaps prevent aortic rupture by maintaining SMC contractile phenotype.

Masson's trichrome staining further illustrates that *Mgp*$^{-/-}$ vessels are highly remodeled, with acellular areas exhibiting observable increased collagen staining (Figure 4A). Verhoeff-Van Gieson (VVG) staining revealed that the aortas of *Mgp*$^{-/-}$ mice exhibited less robust staining for elastin, and less tortuous fibers, in *Mgp*$^{-/-}$ compared to *Mgp*$^{+/+}$ However, rapamycin did not alter elastin fiber length in *Mgp*$^{-/-}$ mice (Figure 4B). Immunofluorescent staining was used to quantify the SMC contractility markers smooth muscle α-actin (SMA) and myosin heavy chain 11 (MYH11) (38, 39). In *Mgp*$^{+/+}$ we observed no differences in SMA levels between vehicle and rapamycin treatment, nor between *Mgp*$^{+/+}$ the *Mgp*$^{-/-}$ mice treated with vehicle. However, rapamycin treatment slightly, but significantly, increased SMA levels in *Mgp*$^{-/-}$ mice compared to vehicle alone. No differences in MYH11 levels were observed (Figure 4C). As the medial layer is remodeled in the *Mgp*$^{-/-}$ mice, we measured the mitotic marker Ki67 and found that at baseline, Ki67 levels were significantly elevated in *Mgp*$^{-/-}$ aorta while nearly undetectable in the *Mgp*$^{+/+}$. However, rapamycin treatment did not alter Ki67 levels in either of the two genotypes (Figure 4D). Together, these data suggest that rapamycin does not significantly alter the medial remodeling or SMC phenotype in *Mgp*$^{-/-}$ mice aorta.

Rapamycin lowered LC3 staining in *Mgp*$^{-/-}$ aorta but there were no observable changes in autophagy flux.

Autophagy is a ubiquitous process and contributes to bone development and the differentiation of osteoblasts and osteoclasts (40) In the vasculature, autophagy reduces vascular calcification by limiting the release of pro-calcific matrix vesicles (41). LC3 is a protein that functions at the initiation of autophagosome formation and serves as an autophagy marker. While there were no differences between the LC3 signal in *Mgp*$^{+/+}$ and *Mgp*$^{-/-}$ at baseline, we observed that rapamycin treatment significantly lowered LC3 puncta in *Mgp*$^{-/-}$ compared to *Mgp*$^{+/+}$ mice (Figure 4A).

Quantifying LC3 puncta hints at diminished autophagy but immunofluorescent staining of fixed tissues cannot assess autophagy flux. LC3-I is cleaved to LC3-II when it is incorporated into autophagosomes, but this process is dynamic and LC3-II can also be degraded during autophagy. The comparison of LC3-II to LC3-I in the presence of an autophagy inhibitor like bafilomycin enables autophagy flux observation (42). We isolated SMCs from *Mgp*$^{+/+}$ and *Mgp*$^{-/-}$ mice to evaluate autophagy flux. SMC were treated with vehicle (DMSO) or 200 nM rapamycin for 14h and then with vehicle or 100 uM or the late-phase autophagy inhibitor bafilomycin for 24h. Rapamycin alone did not increase LC3-II levels compared to vehicle controls in either the *Mgp*$^{+/+}$ and *Mgp*$^{-/-}$ SMC. Bafilomycin, an autophagy inhibitor, increased LC3-II levels in both *Mgp*$^{+/+}$ and *Mgp*$^{-/-}$ SMCs compared to their cognate vehicle controls, however the addition of rapamycin did not further alter LC3-II levels compared to bafilomycin (Figure 5B, left graph). Comparing LC3-II to LC3-I showed identical trends (Figure 5B, right graph), suggesting that global LC3 levels and flux are similar in *Mgp*$^{+/+}$ and *Mgp*$^{-/-}$ SMCs.

Rapamycin is not protecting the mineralized vasculature in *Mgp-/-* mice.

Figure 2 shows that rapamycin treatment doubles the lifespan of *Mgp*$^{-/-}$ mice compared to vehicle alone. However, our subsequent inquiries revealed that rapamycin did not decrease the volume of calcification, did not reverse the adverse remodeling of the medial layer, did not enhance SMC contractile phenotype, or did not induce more autophagy. The mammalian target of rapamycin, mTOR, can form two different protein complexes known as mTORC1, bound to Raptor, and mTORC2, bound to Rictor. The former is acutely sensitive to rapamycin administration, while the latter requires chronic rapamycin dosing for inhibition (19). To investigate whether rapamycin's effect on the *Mgp*$^{-/-}$ mouse are acting on the vasculature, we generated *Mgp*$^{-/-}$ mice with SMC-specific deletion of the mTOR complex proteins Raptor and Rictor (26-28). *Mgp*$^{-/-}$*;Myh11Cre-GFP;Raptor*$^{f/f}$ mice (*Mgp*$^{-/-}$*;Raptor*$^{SMC-/-}$) were bred to examine the effects of a nonfunctional mTORC1 complex, while *Mgp*$^{-/-}$*;Myh11Cre-GFP;Rictor*$^{f/f}$ (*Mgp*$^{-/-}$*;Rictor*$^{SMC-/-}$*)* mice knockout was bred to examine a nonfunctional mTORC2 complex. Fully differentiated SMCs expressing *Myh11* will constitutively express Cre recombinase to inactive *Raptor* and *Rictor* gene expression specifically in SMCs.

Similar to *Mgp*$^{-/-}$ mice treated with vehicle in Figure 2, Figure 6 shows that only 50% of the *Mgp*$^{-/-}$*;Rictor*$^{SMC-/-}$ and *Mgp*$^{-/-}$*;Rictor*$^{SMC+/+}$ are alive at 40 days, indicating that rapamycin acting via mTORC2 does not recapitulate the effects of rapamycin on increasing *Mgp*$^{-/-}$ mice lifespan. The 50% survival rate of *Mgp*$^{-/-}$*;Raptor*$^{SMC+/+}$ mice was similar to *Mgp*$^{-/-}$ treated with vehicle, *Mgp*$^{-/-}$*;Rictor*$^{SMC-/-}$ and *Mgp*$^{-/-}$*;Rictor*$^{SMC+/+}$*,* however the 50% survival rate of MGP$^{-/-}$;Raptor$^{SMC-/-}$ mice dropped to 22 days. As the Cre strain being used is a non-inducible system, this data in the MGP$^{-/-}$;Raptor$^{SMC-/-}$ mice suggest that mTORC1 is critical to the growth and development of the vasculature. Together, these in vivo data suggest that the life-extending effects of rapamycin in the *Mgp*$^{-/-}$ mouse are not acting to preserve or reverse the calcification or deleterious vascular remodeling but are acting on another organ system in the animal.

DISCUSSION

In this study, we demonstrated that rapamycin treatment increased the lifespan in *Mgp*$^{-/-}$ mice, but the effects of rapamycin do not reduce MAC nor rescue vessel integrity. In mice, rapamycin has been shown to increase maximum lifespan and delay the onset of cancer as hyperactivity of the mTOR pathway, frequently found in cancers, leads to the expression and activation of many oncogenes like PI3K, Akt, and eIF4E. Hence, rapamycin can slow the proliferation of tumor cells by causing cell arrest, promoting apoptosis, and blocking angiogenesis in tumor growths (43). However, our data show that the increase in lifespan observed in *Mgp*$^{-/-}$ mice following rapamycin treatment is not associated with improvements in SMC contractile protein expression or enhanced autophagy flux.

While rapamycin is known to inhibit SMC proliferation and is used as such in drug-eluting stents, there is limited research on the effects of rapamycin on vascular morphology in the presence of calcification (36, 44). It was previously shown that treatment with rapamycin limits the progression of abdominal and thoracic aortic aneurysms in mice and preserves elastic lamina integrity (45, 46). In a hyperphosphatemic rat model, rapamycin treatment inhibited aortic calcium deposition when ectopic calcification was induced by feeding the rats with a high-phosphate, high-adenine diet. Rapamycin reduced the osteogenic markers MSX2 and OSX in this model while increasing the *Opn* and *Acta2* gene expression via Klotho upregulation (47). Our approached used a genetic model of MAC to investigate whether rapamycin could inhibit calcification in vivo. MGP-deficient mice develop normally and at the time of birth are without any overt abnormalities. At approximately one week old *Mgp*$^{-/-}$ mice start exhibiting calcification of the vessels, suggesting that other gene products might compensate to prevent calcification

during development and immediately post-birth (16). These observations highlight the differences between genetically induced MAC and high phosphate feeding models. Diet-induced calcification must overcome the effect of endogenous MGP, which is a potent inhibitor of calcification, while the genetic removal of MGP results in calcification from the circulating calcium and phosphate and activation of BMP signaling (12, 14).

Rapamycin has also been shown to preserve the differentiated phenotype of vascular SMCs through IRS-1/P3K/AKT2 pathway (37). Our study did not observe rapamycin enhancing the SMC contractile phenotype in *Mgp*$^{-/-}$ mice. *Sma* expression typically occurs earlier than *Myh11* expression during SMC development, even in undifferentiated mesenchymal cells, and its expression persists throughout the differentiation process (48). In contrast, *Myh11* expression occurs later, during the maturation of SMCs. The first study related to SMC contractile gene expression in response to rapamycin was performed in vitro (37), while our study looked at SMC contractile markers in vivo. Further, the presence of calcification activates mechanosensing pathways that once activated may prevent full re-expression SMC contractile markers (49). However, further investigation would be needed to elucidate how these mechanisms are operating in the context of the *Mgp*$^{-/-}$ mouse.

MAC is characterized by mineral deposits in the medial vessel layer and frequently occurs in patients with PAD. Vascular calcification is an active biological process with many driving forces, including osteogenic dedifferentiation of SMCs, inflammatory signals, hyperphosphatemia, and extracellular matrix remodeling. In this study, rapamycin prolonged the lifespan of mice who developed serious MAC shortly after birth. Interestingly, even though rapamycin stimulates the cellular process of autophagy (50),-which can recycle components of the ECM, including mineral deposits (51)- calcification volume was not reduced in rapamycin treated *Mgp*$^{-/-}$ mice. However, microCT data showed that the mineral density was significantly reduced in *Mgp*$^{-/-}$ mice treated with rapamycin. This data perhaps suggests that changes in mineral structure, if explored at a further timepoint, may impact calcification volume. Alternatively, as MGP also functions to inhibit BMP2 signaling, rapamycin may not interfere with that process- such that changes in dosage or duration of rapamycin treatment would still not alter calcification content in the vessel wall. Another explanation is that the activated autophagy pathways cannot overcome the rapid deposition of hydroxyapatite that occurs in *Mgp*$^{-/-}$ mice. Frauscher et al. demonstrated that induction of autophagy by rapamycin treatment decreased calcification in the vasculature of uremic DBA/2 mice (52). This argument led us to examine autophagy flux in SMCs. However, we did not observe a difference in autophagy flux between *Mgp*$^{+/+}$ and *Mgp*$^{-/-}$. It is important to note that the *Mgp*$^{-/-}$ is on a C57BL6J background, perhaps explaining the differences observed in these in vivo models.

The mammalian target of rapamycin (mTOR) forms two distinct protein complexes known as mTORC1 and mTORC2. mTORC1, activated by amino acids and allosterically inhibited by rapamycin, requires a complex specific protein named raptor (53). After chronic administration, mTORC2 is only inhibited by rapamycin and requires a Rictor (54). In the *Mgp*$^{-/-}$*;Raptor*$^{SMC-/-}$ mice, induction of Cre to knockout *Raptor* was more lethal than the *Mgp*$^{-/-}$*;Raptor*$^{SMC+/+}$ or *Mgp-/-* mice. Therefore, *Raptor* is essential for the growth and maintenance of SMCs in the vasculature. This essential role in growth and development is perhaps unsurprising, considering that global *Raptor* knockout mice die in utero (55). Moreover, there was no benefit to lifespan in the the *Mgp*$^{-/-}$:Rictor$^{SMC-/-}$ mice. The survival curves for the the *Mgp*$^{-/-}$*:Rictor*$^{SMC+/+}$ and *Mgp*$^{-/-}$*;Rictor*$^{SMC-/-}$ mice, targeting mTORC2 signaling, do not diverge at any point and are statistically insignificant, and also mirror that seen in the *Mgp*$^{-/-}$ strain. Considering these data together, rapamycin likely extends the lifespan of *Mgp*$^{-/-}$ mice by targeting another organ system.

Arterial stiffness is strongly linked to heart failure (56), and these non-atherosclerotic vascular pathologies are much more common in some populations, such as African-ancestry individuals who are known to have a higher risk of cardiovascular disease events and mortality compared to Caucasians(57-61). This excess cardiovascular disease risk is largely due to hypertensive and peripheral vascular disease, versus atherosclerotic disease (57-59, 62-64). As such, it is critical to define drivers of MAC such as MGP, which in some clinical studies in humans has been associated with heart failure and MAC (65). Impairment in MGP activation, which would phenocopy genetic deletion, is linked to a higher risk of heart failure and peripheral artery disease due to excessive pulsatile afterloads on the left ventricle that reduce coronary artery perfusion pressure during diastole (66, 67). As the mice that lack MGP are prone to aortic rupture or heart failure, we speculate that rapamycin's effect on the mice's lifespan may be due to rapamycin acting on the cardiac tissues.

Our study suggests that rapamycin's life-extending benefit in *Mgp*$^{-/-}$ mice may act through another organ system, possibly the heart rather than the vessels. Future studies are needed to examine the impact of rapamycin on cardiac function in *Mgp*$^{-/-}$ mice. Rapamycin has been shown to increase cardiomyocyte autophagy (68), limit cardiomyocyte death, and attenuate cardiomyocyte hypertrophy and cardiac remodeling by enhancing mTORC2 signaling while simultaneously inhibiting mTORC1 signaling (69). Inhibition of mTOR signaling with rapamycin improved cardiac function, such as left ventricular end-systolic dimensions, fractional shortening, and ejection fraction in mice with decompensated cardiac hypertrophy compared to the control group (70). Rapamycin has a protective effect on cardiac muscle contractility. Cardiomyocytes isolated from the oldest mice treated with rapamycin show better contraction (similar to that of young mice) than cardiomyocytes from old mice not treated with rapamycin (71).

CONCLUSION

Rapamycin injection extended the lifespan of *Mgp*$^{-/-}$ mice that exhibit an advanced form of MAC compared to *Mgp*$^{+/+}$ mice treated with vehicle, indicating a potential therapeutic benefit. However, the mechanism of rapamycin-induced lifespan in relation to MAC must be clarified. Rapamycin reduced mineral density but did not decrease calcification volume or show any improvement in maintaining the SMC contractile phenotype in *Mgp*$^{-/-}$ mice. Rapamycin did not alter proliferation in either *Mgp*$^{+/+}$ or *Mgp*$^{-/-}$ mice or induce autophagy. The rapamycin effect on lifespan extension and mineral density reduction is independent of its inhibition of mTORC1 or mTORC2 complexes in SMC, suggesting that it is not vascular dysfunction itself leading to death. Thus, we predict that rapamycin is acting on the heart tissue to withstand failure due to the stiffened, calcified vessels.

ACKNOWLEDGEMENTS

We want to thank the Center for Biologic Imaging at the University of Pittsburgh for their help and support with microscopy imaging. Some figures were created with Biorender.com.

SOURCES OF FUNDING

This publication was supported by the NIH K22 HL117917-01A1, The Winters Foundation, The McKamish Family Foundation (St. Hilaire), and the American Heart Association 24POST1186619 (Behzadi). MicorCT analysis and processing was performed on a system supported by NIH S10-OD021533 (Verdelis).

DISCLOSURES

None.

REFERENCES

1. **St. Hilaire C**. Medial Arterial Calcification: A Significant and Independent Contributor of Peripheral Artery Disease. *Arteriosclerosis, Thrombosis, and Vascular Biology* 42: 253-260, 2022.
2. **O'Neill WC, Han KH, Schneider TM, and Hennigar RA**. Prevalence of nonatheromatous lesions in peripheral arterial disease. *Arterioscler Thromb Vasc Biol* 35: 439-447, 2015.
3. **Narula N, Dannenberg AJ, Olin JW, Bhatt DL, Johnson KW, Nadkarni G, Min J, Torii S, Poojary P, Anand SS, Bax JJ, Yusuf S, Virmani R, and Narula J**. Pathology of Peripheral Artery Disease in Patients With Critical Limb Ischemia. *J Am Coll Cardiol* 72: 2152-2163, 2018.
4. **Markello TC, Pak LK, St Hilaire C, Dorward H, Ziegler SG, Chen MY, Chaganti K, Nussbaum RL, Boehm M, and Gahl WA**. Vascular pathology of medial arterial calcifications in NT5E deficiency: implications for the role of adenosine in pseudoxanthoma elasticum. *Mol Genet Metab* 103: 44-50, 2011.
5. **Lanzer P, Hannan FM, Lanzer JD, Janzen J, Raggi P, Furniss D, Schuchardt M, Thakker R, Fok PW, Saez-Rodriguez J, Millan A, Sato Y, Ferraresi R, Virmani R, and St Hilaire C**. Medial Arterial Calcification: JACC State-of-the-Art Review. *J Am Coll Cardiol* 78: 1145-1165, 2021.
6. **Hortells L, Sur S, and St Hilaire C**. Cell Phenotype Transitions in Cardiovascular Calcification. *Front Cardiovasc Med* 5: 27, 2018.
7. **Villa-Bellosta R**. Role of the extracellular ATP/pyrophosphate metabolism cycle in vascular calcification. *Purinergic Signal* 19: 345-352, 2023.
8. **Rutsch F, Ruf N, Vaingankar S, Toliat MR, Suk A, Hohne W, Schauer G, Lehmann M, Roscioli T, Schnabel D, Epplen JT, Knisely A, Superti-Furga A, McGill J, Filippone M, Sinaiko AR, Vallance H, Hinrichs B, Smith W, Ferre M, Terkeltaub R, and Nurnberg P**. Mutations in ENPP1 are associated with 'idiopathic' infantile arterial calcification. *Nat Genet* 34: 379-381, 2003.
9. **St Hilaire C, Ziegler SG, Markello TC, Brusco A, Groden C, Gill F, Carlson-Donohoe H, Lederman RJ, Chen MY, Yang D, Siegenthaler MP, Arduino C, Mancini C, Freudenthal B, Stanescu HC, Zdebik AA, Chaganti RK, Nussbaum RL, Kleta R, Gahl WA, and Boehm M**. NT5E mutations and arterial calcifications. *N Engl J Med* 364: 432-442, 2011.
10. **Baral A, F FH, Lee SC, Matthew BP, Ferrante EA, Brofferio A, Cudrici CD, Rollison SF, Chen MY, Boehm M, and Wen H**. Images in Vascular Medicine: High-resolution CT imaging of arterial calcification in the hands and legs of patients with CD73 deficiency. *Vasc Med* 29: 342-344, 2024.
11. **Jin H, St Hilaire C, Huang Y, Yang D, Dmitrieva NI, Negro A, Schwartzbeck R, Liu Y, Yu Z, Walts A, Davaine JM, Lee DY, Donahue D, Hsu KS, Chen J, Cheng T, Gahl W, Chen G, and Boehm M**. Increased activity of TNAP compensates for reduced adenosine production and promotes ectopic calcification in the genetic disease ACDC. *Sci Signal* 9: ra121, 2016.
12. **Murshed M, Schinke T, McKee MD, and Karsenty G**. Extracellular matrix mineralization is regulated locally; different roles of two gla-containing proteins. *J Cell Biol* 165: 625-630, 2004.
13. **Hackeng TM, Rosing J, Spronk HM, and Vermeer C**. Total chemical synthesis of human matrix Gla protein. *Protein Sci* 10: 864-870, 2001.
14. **Zebboudj AF, Imura M, and Bostrom K**. Matrix GLA protein, a regulatory protein for bone morphogenetic protein-2. *J Biol Chem* 277: 4388-4394, 2002.
15. **Malhotra R, Burke MF, Martyn T, Shakartzi HR, Thayer TE, O'Rourke C, Li P, Derwall M, Spagnolli E, Kolodziej SA, Hoeft K, Mayeur C, Jiramongkolchai P, Kumar R, Buys ES, Yu PB, Bloch KD, and Bloch DB**. Inhibition of bone morphogenetic protein signal

transduction prevents the medial vascular calcification associated with matrix Gla protein deficiency. *PLoS One* 10: e0117098, 2015.

16. **Luo G, Ducy P, McKee MD, Pinero GJ, Loyer E, Behringer RR, and Karsenty G**. Spontaneous calcification of arteries and cartilage in mice lacking matrix GLA protein. *Nature* 386: 78-81, 1997.

17. **Haissaguerre M, Saucisse N, and Cota D**. Influence of mTOR in energy and metabolic homeostasis. *Mol Cell Endocrinol* 397: 67-77, 2014.

18. **Saxton RA, and Sabatini DM**. mTOR Signaling in Growth, Metabolism, and Disease. *Cell* 168: 960-976, 2017.

19. **Panwar V, Singh A, Bhatt M, Tonk RK, Azizov S, Raza AS, Sengupta S, Kumar D, and Garg M**. Multifaceted role of mTOR (mammalian target of rapamycin) signaling pathway in human health and disease. *Signal Transduct Target Ther* 8: 375, 2023.

20. **Arriola Apelo SI, and Lamming DW**. Rapamycin: An InhibiTOR of Aging Emerges From the Soil of Easter Island. *J Gerontol A Biol Sci Med Sci* 71: 841-849, 2016.

21. **Zhan JK, Wang YJ, Wang Y, Wang S, Tan P, Huang W, and Liu YS**. The mammalian target of rapamycin signalling pathway is involved in osteoblastic differentiation of vascular smooth muscle cells. *Can J Cardiol* 30: 568-575, 2014.

22. **He HQ, Law BYK, Zhang N, Qiu CL, Qu YQ, Wu AG, Han Y, Song Q, Zheng WL, Liu Y, He YZ, and Wong VKW**. Bavachin Protects Human Aortic Smooth Muscle Cells Against beta-Glycerophosphate-Mediated Vascular Calcification and Apoptosis via Activation of mTOR-Dependent Autophagy and Suppression of beta-Catenin Signaling. *Front Pharmacol* 10: 1427, 2019.

23. **Dai XY, Zhao MM, Cai Y, Guan QC, Zhao Y, Guan Y, Kong W, Zhu WG, Xu MJ, and Wang X**. Phosphate-induced autophagy counteracts vascular calcification by reducing matrix vesicle release. *Kidney Int* 83: 1042-1051, 2013.

24. **Joolharzadeh P, and St Hilaire C**. CD73 (Cluster of Differentiation 73) and the Differences Between Mice and Humans. *Arterioscler Thromb Vasc Biol* 39: 339-348, 2019.

25. **Ziegler SG, Ferreira CR, MacFarlane EG, Riddle RC, Tomlinson RE, Chew EY, Martin L, Ma CT, Sergienko E, Pinkerton AB, Millan JL, Gahl WA, and Dietz HC**. Ectopic calcification in pseudoxanthoma elasticum responds to inhibition of tissue-nonspecific alkaline phosphatase. *Sci Transl Med* 9: 2017.

26. **Xin HB, Deng KY, Rishniw M, Ji G, and Kotlikoff MI**. Smooth muscle expression of Cre recombinase and eGFP in transgenic mice. *Physiol Genomics* 10: 211-215, 2002.

27. **Sengupta S, Peterson TR, Laplante M, Oh S, and Sabatini DM**. mTORC1 controls fasting-induced ketogenesis and its modulation by ageing. *Nature* 468: 1100-1104, 2010.

28. **Magee JA, Ikenoue T, Nakada D, Lee JY, Guan KL, and Morrison SJ**. Temporal changes in PTEN and mTORC2 regulation of hematopoietic stem cell self-renewal and leukemia suppression. *Cell Stem Cell* 11: 415-428, 2012.

29. **Liu M, Espinosa-Diez C, Mahan S, Du M, Nguyen AT, Hahn S, Chakraborty R, Straub AC, Martin KA, Owens GK, and Gomez D**. H3K4 di-methylation governs smooth muscle lineage identity and promotes vascular homeostasis by restraining plasticity. *Dev Cell* 56: 2765-2782 e2710, 2021.

30. **Wanjare M, Kuo F, and Gerecht S**. Derivation and maturation of synthetic and contractile vascular smooth muscle cells from human pluripotent stem cells. *Cardiovasc Res* 97: 321-330, 2013.

31. **Zhang L, Yang C, Li J, Zhu Y, and Zhang X**. High extracellular magnesium inhibits mineralized matrix deposition and modulates intracellular calcium signaling in human bone marrow-derived mesenchymal stem cells. *Biochem Biophys Res Commun* 450: 1390-1395, 2014.

32. **Schneider CA, Rasband WS, and Eliceiri KW**. NIH Image to ImageJ: 25 years of image analysis. *Nat Methods* 9: 671-675, 2012.

33. **Li Q, Price TP, Sundberg JP, and Uitto J**. Juxta-articular joint-capsule mineralization in CD73 deficient mice: similarities to patients with NT5E mutations. *Cell Cycle* 13: 2609-2615, 2014.
34. **Harrison DE, Strong R, Sharp ZD, Nelson JF, Astle CM, Flurkey K, Nadon NL, Wilkinson JE, Frenkel K, Carter CS, Pahor M, Javors MA, Fernandez E, and Miller RA**. Rapamycin fed late in life extends lifespan in genetically heterogeneous mice. *Nature* 460: 392-395, 2009.
35. **Martin KA, Rzucidlo EM, Merenick BL, Fingar DC, Brown DJ, Wagner RJ, and Powell RJ**. The mTOR/p70 S6K1 pathway regulates vascular smooth muscle cell differentiation. *Am J Physiol Cell Physiol* 286: C507-517, 2004.
36. **Marx SO, Jayaraman T, Go LO, and Marks AR**. Rapamycin-FKBP inhibits cell cycle regulators of proliferation in vascular smooth muscle cells. *Circ Res* 76: 412-417, 1995.
37. **Martin KA, Merenick BL, Ding M, Fetalvero KM, Rzucidlo EM, Kozul CD, Brown DJ, Chiu HY, Shyu M, Drapeau BL, Wagner RJ, and Powell RJ**. Rapamycin promotes vascular smooth muscle cell differentiation through insulin receptor substrate-1/phosphatidylinositol 3-kinase/Akt2 feedback signaling. *J Biol Chem* 282: 36112-36120, 2007.
38. **Cheung C, Bernardo AS, Trotter MW, Pedersen RA, and Sinha S**. Generation of human vascular smooth muscle subtypes provides insight into embryological origin-dependent disease susceptibility. *Nat Biotechnol* 30: 165-173, 2012.
39. **Skalli O, Pelte MF, Peclet MC, Gabbiani G, Gugliotta P, Bussolati G, Ravazzola M, and Orci L**. Alpha-smooth muscle actin, a differentiation marker of smooth muscle cells, is present in microfilamentous bundles of pericytes. *J Histochem Cytochem* 37: 315-321, 1989.
40. **Qi M, Zhang L, Ma Y, Shuai Y, Li L, Luo K, Liu W, and Jin Y**. Autophagy Maintains the Function of Bone Marrow Mesenchymal Stem Cells to Prevent Estrogen Deficiency-Induced Osteoporosis. *Theranostics* 7: 4498-4516, 2017.
41. **Sun X, Zheng Y, Xie L, Zhou Y, Liu R, Ma Y, Zhao M, and Liu Y**. Autophagy reduces aortic calcification in diabetic mice by reducing matrix vesicle body-mediated IL-1beta release. *Exp Cell Res* 432: 113803, 2023.
42. **Mizushima N, and Yoshimori T**. How to Interpret LC3 Immunoblotting. *Autophagy* 3: 542-545, 2014.
43. **Ganesh SK, and Subathra Devi C**. Molecular and therapeutic insights of rapamycin: a multi-faceted drug from Streptomyces hygroscopicus. *Mol Biol Rep* 50: 3815-3833, 2023.
44. **Sabate M**. Sirolimus Versus Paclitaxel: Second Round. *JACC Cardiovasc Interv* 15: 780-782, 2022.
45. **Rouer M, Xu BH, Xuan HJ, Tanaka H, Fujimura N, Glover KJ, Furusho Y, Gerritsen M, and Dalman RL**. Rapamycin limits the growth of established experimental abdominal aortic aneurysms. *Eur J Vasc Endovasc Surg* 47: 493-500, 2014.
46. **Zhou B, Li W, Zhao G, Yu B, Ma B, Liu Z, Xie N, Fu Y, Gong Z, Dai R, Zhang X, and Kong W**. Rapamycin prevents thoracic aortic aneurysm and dissection in mice. *J Vasc Surg* 69: 921-932 e923, 2019.
47. **Zhao Y, Zhao MM, Cai Y, Zheng MF, Sun WL, Zhang SY, Kong W, Gu J, Wang X, and Xu MJ**. Mammalian target of rapamycin signaling inhibition ameliorates vascular calcification via Klotho upregulation. *Kidney Int* 88: 711-721, 2015.
48. **Li L, Miano JM, Cserjesi P, and Olson EN**. SM22α, a Marker of Adult Smooth Muscle, Is Expressed in Multiple Myogenic Lineages During Embryogenesis. *Circulation Research* 78: 188-195, 1996.
49. **Krohn JB, Hutcheson JD, Martínez-Martínez E, Irvin WS, Bouten CVC, Bertazzo S, Bendeck MP, and Aikawa E**. Discoidin Domain Receptor-1 Regulates Calcific Extracellular Vesicle Release in Vascular Smooth Muscle Cell Fibrocalcific Response via Transforming Growth Factor-β Signaling. *Arteriosclerosis Thrombosis and Vascular Biology* 36: 525-533, 2016.

50. **Tanemura M, Ohmura Y, Deguchi T, Machida T, Tsukamoto R, Wada H, Kobayashi S, Marubashi S, Eguchi H, Ito T, Nagano H, Mori M, and Doki Y**. Rapamycin causes upregulation of autophagy and impairs islets function both in vitro and in vivo. *Am J Transplant* 12: 102-114, 2012.
51. **Duan ZX, Tu C, Liu Q, Li SQ, Li YH, Xie P, and Li ZH**. Adiponectin receptor agonist AdipoRon attenuates calcification of osteoarthritis chondrocytes by promoting autophagy. *J Cell Biochem* 121: 3333-3344, 2020.
52. **Frauscher B, Kirsch AH, Schabhuttl C, Schweighofer K, Ketszeri M, Pollheimer M, Dragun D, Schroder K, Rosenkranz AR, Eller K, and Eller P**. Autophagy Protects From Uremic Vascular Media Calcification. *Front Immunol* 9: 1866, 2018.
53. **Szwed A, Kim E, and Jacinto E**. Regulation and metabolic functions of mTORC1 and mTORC2. *Physiol Rev* 101: 1371-1426, 2021.
54. **Sarbassov DD, Ali SM, Sengupta S, Sheen JH, Hsu PP, Bagley AF, Markhard AL, and Sabatini DM**. Prolonged rapamycin treatment inhibits mTORC2 assembly and Akt/PKB. *Mol Cell* 22: 159-168, 2006.
55. **Guertin DA, Stevens DM, Thoreen CC, Burds AA, Kalaany NY, Moffat J, Brown M, Fitzgerald KJ, and Sabatini DM**. Ablation in mice of the mTORC components raptor, rictor, or mLST8 reveals that mTORC2 is required for signaling to Akt-FOXO and PKCalpha, but not S6K1. *Dev Cell* 11: 859-871, 2006.
56. **Schott A, Kluttig A, Mikolajczyk R, Greiser KH, Werdan K, Sedding D, and Nuding S**. Association of arterial stiffness and heart failure with preserved ejection fraction in the elderly population - results from the CARLA study. *J Hum Hypertens* 37: 463-471, 2023.
57. **Writing Group M, Lloyd-Jones D, Adams RJ, Brown TM, Carnethon M, Dai S, De Simone G, Ferguson TB, Ford E, Furie K, Gillespie C, Go A, Greenlund K, Haase N, Hailpern S, Ho PM, Howard V, Kissela B, Kittner S, Lackland D, Lisabeth L, Marelli A, McDermott MM, Meigs J, Mozaffarian D, Mussolino M, Nichol G, Roger VL, Rosamond W, Sacco R, Sorlie P, Roger VL, Thom T, Wasserthiel-Smoller S, Wong ND, Wylie-Rosett J, American Heart Association Statistics C, and Stroke Statistics S**. Heart disease and stroke statistics--2010 update: a report from the American Heart Association. *Circulation* 121: e46-e215, 2010.
58. **Allison MA, Ho E, Denenberg JO, Langer RD, Newman AB, Fabsitz RR, and Criqui MH**. Ethnic-specific prevalence of peripheral arterial disease in the United States. *Am J Prev Med* 32: 328-333, 2007.
59. **Allison MA, Budoff MJ, Nasir K, Wong ND, Detrano R, Kronmal R, Takasu J, and Criqui MH**. Ethnic-specific risks for atherosclerotic calcification of the thoracic and abdominal aorta (from the Multi-Ethnic Study of Atherosclerosis). *Am J Cardiol* 104: 812-817, 2009.
60. **Chaturvedi N, Bulpitt CJ, Leggetter S, Schiff R, Nihoyannopoulos P, Strain WD, Shore AC, and Rajkumar C**. Ethnic differences in vascular stiffness and relations to hypertensive target organ damage. *J Hypertens* 22: 1731-1737, 2004.
61. **D'Agostino RB, Jr., Burke G, O'Leary D, Rewers M, Selby J, Savage PJ, Saad MF, Bergman RN, Howard G, Wagenknecht L, and Haffner SM**. Ethnic differences in carotid wall thickness. The Insulin Resistance Atherosclerosis Study. *Stroke* 27: 1744-1749, 1996.
62. **Ali H, Zmuda JM, Cvejkus RK, Kershaw EE, Kuipers AL, Oczypok EA, Wheeler V, Bunker CH, and Miljkovic I**. Wnt Pathway Inhibitor DKK1: A Potential Novel Biomarker for Adiposity. *J Endocr Soc* 3: 488-495, 2019.
63. **Bild DE, Detrano R, Peterson D, Guerci A, Liu K, Shahar E, Ouyang P, Jackson S, and Saad MF**. Ethnic differences in coronary calcification: the Multi-Ethnic Study of Atherosclerosis (MESA). *Circulation* 111: 1313-1320, 2005.
64. **Budoff MJ, Nasir K, Mao S, Tseng PH, Chau A, Liu ST, Flores F, and Blumenthal RS**. Ethnic differences of the presence and severity of coronary atherosclerosis. *Atherosclerosis* 187: 343-350, 2006.

65. **Malhotra R, Nicholson CJ, Wang D, Bhambhani V, Paniagua S, Slocum C, Sigurslid HH, Lino Cardenas CL, Li R, Boerboom SL, Chen YC, Hwang SJ, Yao C, Ichinose F, Bloch DB, Lindsay ME, Lewis GD, Aragam JR, Hoffmann U, Mitchell GF, Hamburg NM, Vasan RS, Benjamin EJ, Larson MG, Zapol WM, Cheng S, Roh JD, O'Donnell CJ, Nguyen C, Levy D, and Ho JE**. Matrix Gla Protein Levels Are Associated With Arterial Stiffness and Incident Heart Failure With Preserved Ejection Fraction. *Arterioscler Thromb Vasc Biol* 42: e61-e73, 2022.

66. **Dalmeijer GW, van der Schouw YT, Magdeleyns EJ, Vermeer C, Verschuren WM, Boer JM, and Beulens JW**. Matrix Gla protein species and risk of cardiovascular events in type 2 diabetic patients. *Diabetes Care* 36: 3766-3771, 2013.

67. **Chirinos JA**. Matrix Gla Protein, Large Artery Stiffness, and the Risk of Heart Failure With Preserved Ejection Fraction. *Arterioscler Thromb Vasc Biol* 42: 223-226, 2022.

68. **Buss SJ, Muenz S, Riffel JH, Malekar P, Hagenmueller M, Weiss CS, Bea F, Bekeredjian R, Schinke-Braun M, Izumo S, Katus HA, and Hardt SE**. Beneficial effects of Mammalian target of rapamycin inhibition on left ventricular remodeling after myocardial infarction. *J Am Coll Cardiol* 54: 2435-2446, 2009.

69. **Volkers M, Konstandin MH, Doroudgar S, Toko H, Quijada P, Din S, Joyo A, Ornelas L, Samse K, Thuerauf DJ, Gude N, Glembotski CC, and Sussman MA**. Mechanistic target of rapamycin complex 2 protects the heart from ischemic damage. *Circulation* 128: 2132-2144, 2013.

70. **McMullen JR, Sherwood MC, Tarnavski O, Zhang L, Dorfman AL, Shioi T, and Izumo S**. Inhibition of mTOR signaling with rapamycin regresses established cardiac hypertrophy induced by pressure overload. *Circulation* 109: 3050-3055, 2004.

71. **Chakraborty AD, Kooiker K, Kobak KA, Cheng Y, Lee CF, Razumova M, Granzier HH, Regnier M, Rabinovitch PS, Moussavi-Harami F, and Chiao YA**. Late-life Rapamycin Treatment Enhances Cardiomyocyte Relaxation Kinetics and Reduces Myocardial Stiffness. *bioRxiv* 2023.

FIGURE LEGENDS

Figure 1: Histological comparison of Matrix Gla Protein (*Mgp*) mice arteries, medial and intimal calcification in human arteries. A. Histological sections of *Mgp*$^{-/-}$ mouse aorta, human tibial plaque and human coronary artery with atherosclerotic plaque, stained for calcification using Von Kossa Staining. *Mgp*$^{-/-}$ mouse aorta develop calcification (Calc) in the media layer of artery similar to human tibial artery. **B.** Dot Blot Assay to identify MGP protein in Wild Type (*Mgp*$^{+/+}$), Heterozygous (*Mgp*$^{+/-}$), and Knockout MGP (*Mgp*$^{-/-}$) mice. *Mgp*$^{-/-}$ showed no expression of MGP (Scale Bars: human tissue 1 mm, mouse tissue 0.5 mm).

Figure 2: Impact of rapamycin treatment on survival in Matrix Gla Protein (*Mgp*)-deficient mice A. Kaplan-Meier analysis of overall survival in *Mgp*$^{+/+}$ and *Mgp*$^{-/-}$ mice treated with vehicle (Dimethyl sulfoxide; DMSO) or rapamycin (5mg/kg/week) for 3 months. Rapamycin treatment significantly extends the survival of *Mgp*$^{-/-}$ mice (n=7) compared to those treated with the vehicle (n=19). *Mgp*$^{+/+}$ mice treated with vehicle (n=5) or either rapamycin (n=8) showed the same survival.

Figure 3: Effect of rapamycin treatment on medial calcification in Matrix Gla Protein (*Mgp)*-deficient mice a. A cross-section of the aorta from *Mgp*$^{-/-}$ mice treated with vehicle (Veh) or rapamycin (RAPA, [5 mg/kg] once or three times a week). Mineral density decreased with three times a week rapamycin. **B.** Histological sections of *Mgp*$^{+/+}$ and *Mgp*$^{-/-}$ mouse aortas

763 treated with vehicle or rapamycin three times a week, stained for calcification using Von Kossa
764 staining. **C.** A cross-section of the aorta treated with vehicle or rapamycin three times a week
765 were stained for calcification marker runt-related transcription factor 2 (RUNX2) by
766 immunofluorescence. In *Mgp*$^{-/-}$ mice, RUNX2 expression was elevated with vehicle treatment
767 but no significant difference with rapamycin treatment.
768
769 **Figure 4: Histological structure of *Mgp*$^{+/+}$ and *Mgp*$^{-/-}$ mice aorta treated with**
770 **vehicle or rapamycin. A.** The cross sections of mice aorta were stained with Masson's
771 Trichrome to identify collagen (stained blue). The staining revealed disruption in
772 collagen fiber structure in *Mgp*$^{-/-}$ mice treated either with vehicle or rapamycin **B.** The
773 cross sections of mice aorta were stained with Verhoeff-Van Gieson (VVG) to identify
774 elastic fibers (stained black). The staining revealed disruption of elastic fiber structure
775 and a reduction of elastic fibers in the *Mgp*$^{-/-}$ vehicle (Veh) group, and no difference
776 observed with rapamycin (RAPA) treatment (Scale bar: 0.2 mm). **C.** The cross sections
777 of mice aorta were stained with smooth muscle actin (SMA) and myosin heavy chain
778 gene (MYH11) SMA. The rapamycin increased the SMA levels in *Mgp*$^{-/-}$ mice compared
779 to the *Mgp*$^{-/-}$ vehicle. **D.** The cross section of mice aorta was stained for proliferation
780 markers (ki67), which was higher in *Mgp*$^{-/-}$ compared to the *Mgp*$^{+/+}$.
781
782
783 **Figure 5: The effect of rapamycin treatment on autophagy flux. A.** Histological sections of
784 *Mgp*$^{+/+}$ and *Mgp*$^{-/-}$ mouse aortas treated with vehicle (DMSO, Dimethyl sulfoxide) or rapamycin
785 [5mg/kg] three times a week, stained for Microtubule-associated protein 1A/1B-light chain 3
786 (LC3) by immunofluorescence. LC3 decreased with rapamycin (RAPA) in *Mgp*$^{-/-}$ mice compared
787 to the *Mgp*$^{+/+}$ mice. **B.** Smooth muscle cells from *Mgp*$^{+/+}$ and *Mgp*$^{-/-}$ mice were treated with
788 vehicle (DMSO) or rapamycin (200 µM) for 14 hours, followed by the addition of bafilomycin
789 (BafA, 100 µM), an autophagy inhibitor, for an additional 24 hours. Levels of LC3 (LC3-I and
790 LC3-II) were quantified by western blot. Rapamycin treatment increases the levels of LC3-
791 II/LC3I and LC3-II protein in both *Mgp*$^{+/+}$ and *Mgp*$^{-/-}$ mice smooth muscle cells.
792
793 **Figure 6: Survival probability of Matrix Gla Protein (*Mgp*)-deficient mice with**
794 **Rictor and Raptor knockouts in vascular smooth muscle cells (SMC). A.** *Mgp*$^{-/-}$
795 using Cre recombinase that target the gene encoding Rictor in SMC (SMC$^{+/+}$ (n=7),
796 SMC$^{-/-}$ (n=5)), a protein involved in mTORC2 signaling pathways. **B.** *Mgp*$^{-/-}$ using Cre
797 recombinase that target the gene encoding Raptor in SMC (SMC$^{+/+}$ (n=6), SMC$^{-/-}$ (n=7)),
798 a protein involved in mTORC1 signaling pathways. The presence or absence of Rictor,
799 when combined with MGP deficiency, does not significantly affect the lifespan of the
800 mice. However, Raptor plays a crucial role in the survival of MGP-deficient mice.
801

A

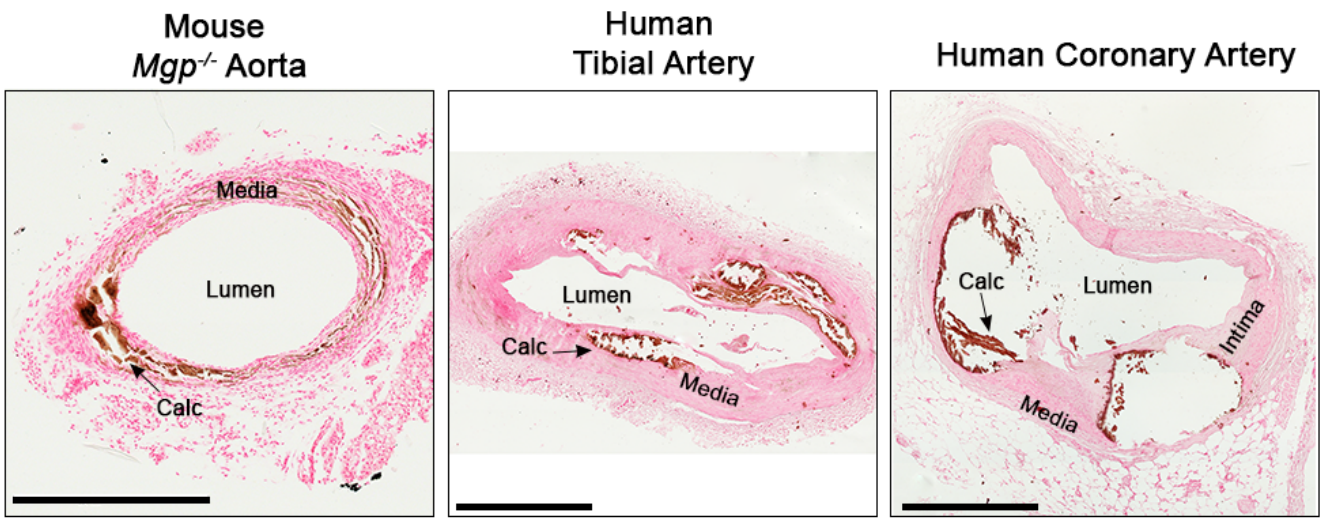

B